

## LYMPHOID NEOPLASIA

## CD30 targeting with brentuximab vedotin: a novel therapeutic approach to primary effusion lymphoma

Shruti Bhatt,<sup>1,2</sup> Brittany M. Ashlock,<sup>3</sup> Yasodha Natkunam,<sup>4</sup> Victoria Sujoy,<sup>5</sup> Jennifer Rose Chapman,<sup>5</sup> Juan Carlos Ramos,<sup>2</sup> Enrique A. Mesri,<sup>3</sup> and Izidore S. Lossos<sup>1,2</sup>

<sup>1</sup>Department of Molecular and Cellular Pharmacology, <sup>2</sup>Department of Medicine, Division of Hematology-Oncology, and <sup>3</sup>Department of Microbiology and Immunology, Sylvester Comprehensive Cancer Center, University of Miami Miller School of Medicine, Miami, FL; <sup>4</sup>Department of Pathology, Stanford University School of Medicine, Stanford, CA; and <sup>5</sup>Department of Pathology, University of Miami Miller School of Medicine, Miami, FL

## Key Points

- Brentuximab vedotin serves as an effective therapy for PEL.
- Brentuximab vedotin led to cytotoxic effects in PEL cell lines and extended survival of xenograft mice.

**Primary effusion lymphoma (PEL) is an aggressive subtype of non-Hodgkin lymphoma characterized by short survival with current therapies, emphasizing the urgent need to develop new therapeutic approaches. Brentuximab vedotin (SGN-35) is an anti-CD30 monoclonal antibody (cAC10) conjugated by a protease-cleavable linker to a microtubule-disrupting agent, monomethyl auristatin E. Brentuximab vedotin is an effective treatment of relapsed CD30-expressing Classical Hodgkin and systemic anaplastic large cell lymphomas. Herein, we demonstrated that PEL cell lines and primary tumors express CD30 and thus may serve as potential targets for brentuximab vedotin therapy. In vitro treatment with brentuximab vedotin decreased cell proliferation, induced cell cycle arrest, and triggered apoptosis of PEL cell lines. Furthermore, in vivo brentuximab**

**vedotin promoted tumor regression and prolonged survival of mice bearing previously reported UM-PEL-1 tumors as well as UM-PEL-3 tumors derived from a newly established and characterized Kaposi's sarcoma-associated herpesvirus- and Epstein-Barr virus-positive PEL cell line. Overall, our results demonstrate for the first time that brentuximab vedotin may serve as an effective therapy for PEL and provide strong preclinical indications for evaluation of brentuximab vedotin in clinical studies of PEL patients. (*Blood*. 2013;122(7):1233-1242)**

## Introduction

Primary effusion lymphoma (PEL) is an aggressive and rare malignancy predominantly occurring in patients with HIV infection and severe immunodeficiency.<sup>1</sup> PEL has also been reported in recipients of solid organ transplants and in elderly patients in the absence of immunodeficiencies. PEL is a distinct subtype of B-cell non-Hodgkin lymphoma (NHL) characterized by lymphomatous effusions within major body cavities (pleural, peritoneal, and pericardial); extracavitary tumors are rare but have been reported and have similar morphologic and phenotypic characteristics.<sup>2</sup> Morphologically, PEL cells range in appearance from large immunoblastic or plasmablastic cells to cells with a more anaplastic morphology.<sup>3</sup> PEL cells may usually express CD45 but lack pan-B-cell markers, including surface and cytoplasmic immunoglobulin (Ig), and frequently harbor clonal Ig rearrangements.<sup>3,4</sup> In addition, PEL cells frequently express activation and terminally differentiated B-cell/plasma cell-related markers (eg, HLA-DR, CD30, CD38, IRF4, and CD138).

Kaposi's sarcoma-associated herpesvirus (KSHV), also known as human herpesvirus-8 (HHV-8), is uniformly detected in PEL cells.<sup>1,5,6</sup> Although KSHV is the main causative agent for PEL, almost 80% of the cases are also co-infected with Epstein-Barr virus (EBV), which may contribute to cell transformation.<sup>2</sup> The majority of PEL cells are latently infected with KSHV and express latency-associated viral proteins, including viral cyclin, viral FADD-like interleukin-1- $\beta$ -converting enzyme inhibitory protein, latency-associated nuclear

antigen (LANA), kaposin, and a group of viral microRNAs.<sup>7</sup> In a very small fraction of infected cells, the virus undergoes lytic replication producing mature virions and cell lysis.<sup>7,8</sup> The lytic replication occurs in a coordinated cascade of immediate early (IE), early, and late genes. IE genes transactivate and promote the expression of early lytic genes, which in turn participate in viral DNA replication. Late lytic genes are expressed after viral DNA replication, allowing mature virion formation and egress from the cells.

PEL displays an aggressive clinical course with a median survival time of only 6 months from diagnosis. Current therapeutic approaches, including combination chemotherapy with cyclophosphamide, doxorubicin, vincristine, and prednisone-like regimens, highly active anti-retroviral therapy, and other antiviral approaches lead to only transient responses and do not cure these patients. Recently, treatment with bortezomib (a proteasome inhibitor) alone<sup>9</sup> or in combination with vorinostat (a histone deacetylase inhibitor, also known as a suberoylanilide hydroxamic acid) has been found to prolong the survival of mice bearing PEL tumors.<sup>10</sup> But the systemic efficacy of these drugs is yet to be evaluated in PEL patients. Overall, there is an urgent need to develop more effective therapeutic approaches to PEL.

Antibody-based therapies have shown remarkable therapeutic activities in various tumors, including rituximab in B-cell lymphoma, trastuzumab in breast cancer, and cetuximab in colorectal cancer. These approaches target specific antigens expressed on the cancerous

Submitted January 29, 2013; accepted June 25, 2013. Prepublished online as *Blood* First Edition paper, July 9, 2013; DOI 10.1182/blood-2013-01-481713.

The online version of this article contains a data supplement.

The publication costs of this article were defrayed in part by page charge payment. Therefore, and solely to indicate this fact, this article is hereby marked "advertisement" in accordance with 18 USC section 1734.

© 2013 by The American Society of Hematology

cells, resulting in increased therapeutic efficacy and minimum systemic toxicity. CD30, a member of the tumor necrosis factor- $\alpha$  receptor family, is highly expressed in specific cancers with limited expression in healthy tissues, thus making it an ideal therapeutic target.<sup>11-14</sup>

Brentuximab vedotin (ADCETRIS, SGN-35) is a novel antibody-drug conjugate in which a chimeric anti-CD30 antibody, cAC10, is combined with the synthetic microtubule-disrupting agent monomethylauristatin E (MMAE) using a protease-cleavable linker.<sup>15,16</sup> Each antibody is conjugated to an average of 4 molecules of MMAE. Upon binding to CD30-expressing neoplastic cells, the antibody-drug conjugate is internalized by endocytosis. Lysosomal degradation causes selective cleavage of the linker, allowing release of the MMAE. The MMAE molecules bind to tubulin, effectively disrupting the microtubule network with resultant cell cycle arrest and apoptosis.<sup>16-18</sup> Recently, brentuximab vedotin demonstrated high response rates as a single agent in clinical trials for relapsed/refractory Hodgkin lymphoma (HL) and anaplastic large cell lymphoma (ALCL),<sup>19,20</sup> leading to its accelerated approval by the Food and Drug Administration for treatment of these lymphomas.<sup>21</sup> In the present study, we show that PEL cell lines and primary PEL tumors express CD30 and can be targeted by brentuximab vedotin, leading to cytotoxic effects in PEL cell lines and prolonged survival of mice bearing PEL xenografts.

## Materials and methods

### Cell lines and reagents

The UM-PEL-1 (KSHV+/EBV+) cell line was previously reported.<sup>9</sup> For in vitro studies, UM-PEL-1 cells collected from mice and established in culture (UM-PEL-1c) were used. UM-PEL-3 was established as described in the "Results" section and UM-PEL-3c refers to cells collected from mice and established in culture. The diffuse large B-cell lymphoma cell line WSU-NHL<sup>22</sup> was obtained from Dr Mohamad Anwar (Wayne State University). The PEL cell lines UM-PEL-1c (KSHV+/EBV+), UM-PEL-3c (KSHV+/EBV+), BC-1 (KSHV+/EBV+), BC-3 (KSHV+/EBV-), and BC-5 (KSHV+/EBV+),<sup>4,23</sup> the Burkitt's lymphoma cell line (Raji), and the ALCL cell lines SUDHL-1, Karpas 299, and SUP-M2 were cultured in RPMI 1640 medium (Mediatech) supplemented with 10% fetal bovine serum (Mediatech) and penicillin/streptomycin (Gibco BRL). Brentuximab vedotin and isotype-matched irrelevant Ig-vMMAE were generously provided by Seattle Genetics. Antibodies for CD45, CD38, and CD138 were purchased from Beckman Coulter. UM-PEL-3c cells are available through the AIDS Cancer Specimen Repository (www.acsr.org) as specimen with ID 2012002.

### CD30 cell surface staining

For cell surface CD30 staining,  $0.1 \times 10^6$  UM-PEL-1c and UM-PEL-3c cells obtained from peritoneal effusions of PEL-bearing mice or BC-1, BC-3, and BC-5 cells grown in vitro were washed with phosphate-buffered saline (PBS), resuspended in cold staining buffer (Hanks' balanced salt solution with 2% fetal bovine serum and 1  $\mu$ g/mL blocker [BD Biosciences]) and incubated for 15 minutes. Fluorescein isothiocyanate-conjugated anti-CD30 antibody (BD Biosciences) or matched isotype control were added for 30 minutes followed by 3 washes and cell resuspension in cold staining buffer. Cells were analyzed on a BD FACS Canto-II analyzer (BD Biosciences). The antigen-binding capacity of brentuximab vedotin is described in the supplemental Material and methods available on the *Blood* website.

### Immunohistochemistry

Serial sections of 4  $\mu$ m were cut and deparaffinized in xylene and hydrated in graded alcohols. Immunohistochemistry for CD30 (clone BerH2, dilution 1:40; Dako) was performed using the Leica Bond-Max automated stainer

(Leica Microsystems, Bannockburn, IL). Immunohistochemistry for CD138 (syndecan-1, clone M115, dilution 1:50; Dako) and LANA protein of HHV-8 (clone 13B10, dilution 1:50; Cell Marque) was performed using the Ventana BenchMarkXT automated stainer (Roche-Ventana Medical Systems). KSHV immunofluorescence is described in the supplemental Material and methods.

### Viability, cell cycle, apoptosis, RNA isolation, and quantitative real-time RT-PCR

The methodologies used for these experiments are described in the supplemental Material and methods.

### In vivo tumor studies

All animal studies were conducted according to an approved Institutional Animal Care and Use Committee protocol. UM-PEL-1 and UM-PEL-3 cells ( $25 \times 10^6$ ) isolated from ascites of tumor-bearing NOD/SCID mice were resuspended in 200  $\mu$ L ascites fluid and injected intraperitoneally into tumor naïve NOD/SCID mice. On day 3, tumor-bearing mice were randomly assigned to PBS (50  $\mu$ L thrice weekly), isotype-matched irrelevant Ig-vMMAE controls (3 mg/kg thrice weekly), or brentuximab vedotin (3 mg/kg thrice weekly) treatment groups. Treatment was given for 3 consecutive weeks. Mice were monitored daily and sacrificed when moribund or exhibiting signs of discomfort. IRB approval was obtained to carry out studies involving human subjects, who gave written consent in accordance with the Declaration of Helsinki.

### Statistical analysis

Statistical significance of the data was determined using the 2-tailed Student *t* test. *P* values < .05 were considered significant. Statistical analysis was performed using Graph Pad Prism 5.0 software. Survival was estimated using the Kaplan-Meier survival curve method and differences in survival were calculated using the long-rank test (Graph Pad Prism). All values are expressed as standard errors of the mean.

## Results

### Establishment and characterization of UM-PEL-3 cell line

Due to the shortage of suitable in vitro and in vivo model systems to study PEL, a new UM-PEL-3 cell line was established from an HIV-positive and hepatitis C-positive 45-year-old male with PEL presenting with large ascites. Establishment of the UM-PEL-3 tumor model in NOD/SCID mice was carried out as previously described for the UM-PEL-1 cell line.<sup>9</sup> Briefly, lymphoma cells obtained from a peritoneal fluid tap of this patient were directly injected into NOD/SCID mice. Flow cytometric immunophenotypic analysis of the lymphoid cells obtained from the diagnostic tap demonstrated that the cells expressed CD45, CD38, CD138, and CD30 on their surface and were positive for HHV-8 using immunofluorescence for the LANA protein and EBV-encoded RNA (supplemental Table 2). These cells were negative for surface CD3, CD19, CD20, and CD79a. Cytogenetic analysis revealed hypotetraploidy with 81-91 chromosomes and numerous structural abnormalities, including rearrangement of 14q32 (supplemental Table 2). At 2 weeks post cell inoculation into mice, peritoneal swelling indicating ascite development was observed and by 3 weeks, cells were harvested for subsequent characterization and propagation in additional animals. Cell propagation in vivo and in vitro did not change the cell immunophenotype as demonstrated by repeated testing (not shown). Furthermore, the cells remained monoclonal, as demonstrated by Ig heavy chain variable region (IGHV) PCR analysis, revealing

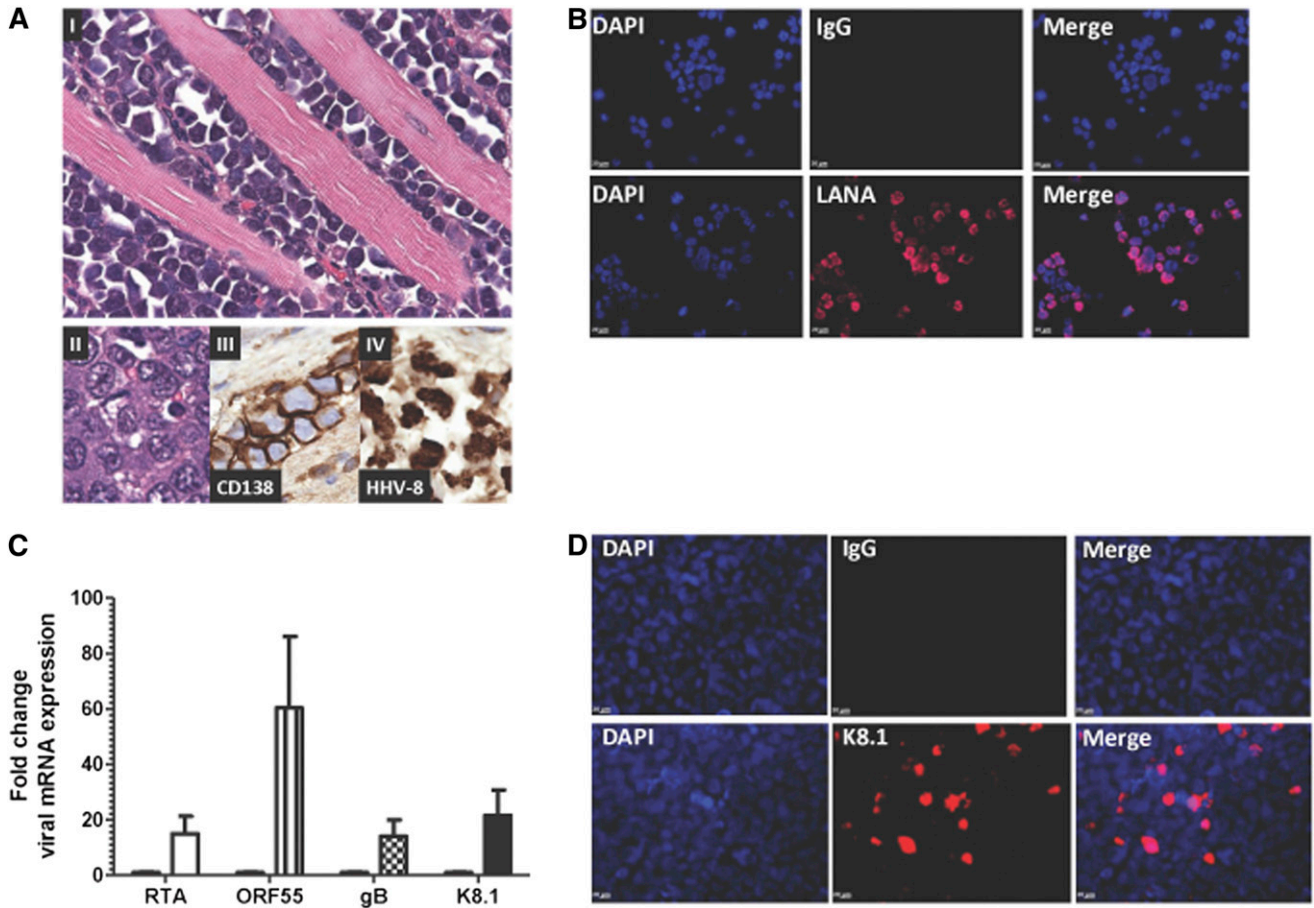


**Figure 1. Characterization of UM-PEL-3 cells.** (A) Pathological findings for the UM-PEL-3 xenograft mouse model. (I-II) Hematoxylin and eosin-stained tissue sections of the gastrointestinal tract showing extensive infiltration of the muscularis propria by lymphoma cells. (II) Higher magnification of pleomorphic lymphoma cells with hyperchromatic nuclei. (III) Immunohistochemistry for CD138 and (IV) HHV8 latent antigen LANA. Original magnification  $\times 400$  (I) and  $\times 600$  (II-IV). (B) IFA of UM-PEL-3 cells reveals positive staining for HHV8 latent antigen LANA (red). (C) UM-PEL-3 cells were stimulated with 1 mM butyrate for 4 days and RNA expression of the indicated transcripts was measured by qRT-PCR. Fold change compared with unstimulated cells indicates induction of IE (RTA), early (ORF55), or late (gB and K8.1) lytic genes. Error bars correspond to standard error of mean. (D) Immunostaining image of late lytic protein K8.1 (red) in UM-PEL-3 cells stimulated with 0.75  $\mu$ M SAHA for 24 hours (bottom) and unstimulated cells (top). For panels B and D, nuclei are stained with 4,6 diamidino-2-phenylindole (DAPI; blue). Magnification  $\times 400$ . Experiments depicted in panels B-D were repeated thrice independently in triplicate. The representative data from one experiment are shown.

a monoclonal rearrangement of the *IGHV4-34* gene with 97% identity to germ line sequence.

Repeated *in vivo* propagation of the UM-PEL-3 cells reproducibly led to the development of PEL ascites accompanied by cellular infiltration into the peritoneum and gastrointestinal tract (Figure 1A I). The UM-PEL-3 cells obtained from an abdominal tap of the mice were positive for CD138 (Figure 1A III) and harbored HHV8 episomes, as evident by immunohistochemistry for the HHV8 LANA nuclear protein (Figure 1A IV).

Immunofluorescence analysis (IFA) showed that UM-PEL-3 cells were positive for LANA (Figure 1B) and displayed the classic nuclear punctuated pattern produced by the staining of LANA at the tethering loci between KSHV episomes and the host chromosomes.<sup>24</sup> Furthermore, lytic induction of KSHV was established by stimulating UM-PEL-3 cells with 40 nM butyrate for 96 hours, followed by quantitative real-time reverse-transcription polymerase chain reaction (qRT-PCR) for lytic viral proteins. qRT-PCR analysis revealed significant upregulation in transcript levels of IE (RTA), early (ORF55), and late lytic genes (gB, K8.1) (Figure 1C). Induction of the late lytic antigen K8.1 at the protein level was confirmed by immunofluorescence staining of the UM-PEL-3 cells stimulated with 0.75  $\mu$ M suberoylanilide hydroxamic acid for 24 hours (Figure 1D).

Infection with EBV was confirmed by PCR analysis of DNA from UM-PEL-3 cells using primers specific for EBV genes EBNA1, LMP1, EBV-encoded RNA 1, and LMP-TK (supplemental Figure 1). Together, these data confirm that UM-PEL-3 cells obtained from peritoneal effusions of tumor-bearing mice are phenotypically similar to the original human PEL cells, harbor EBV and KSHV, and demonstrate the ability to undergo KSHV lytic reactivation.

**CD30 expression in cell lines and primary tumors of PEL**

Cell surface expression of CD30 is reported in a variety of NHLs.<sup>25</sup> Based on the WHO classification of tumors of hematopoietic and lymphoid tissues, PEL cells should express CD30.<sup>26</sup> To confirm CD30 expression on the PEL cell lines, UM-PEL-1, UM-PEL-3, BC-1, BC-3, and BC-5 were stained with an anti-CD30 antibody and analyzed by flow cytometry. As expected, all PEL cell lines tested were found to be positive for CD30, whereas the large B-cell lymphoma cell line, WSU-NHL, was negative as expected (Figure 2A).

UM-PEL-3 cells expressed comparable levels of CD30 as UM-PEL-1 (Figure 1A). To further expand these observations to primary tumors, 9 primary PEL specimens were studied for CD30 expression using immunohistochemistry and/or immunocytochemistry

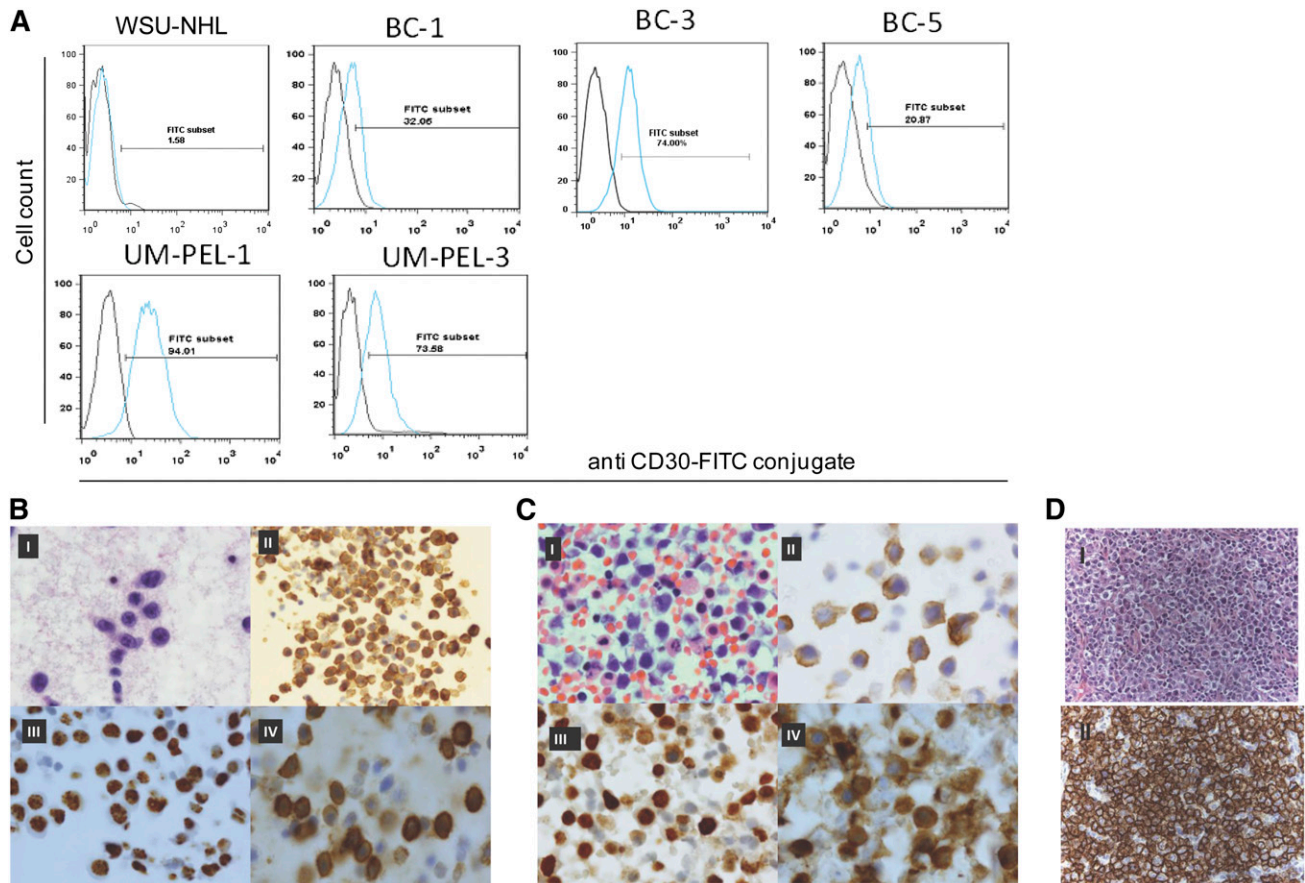


**Figure 2. CD30 expression in PEL cell lines and primary tumors.** (A) Histogram of flow cytometric analysis shows CD30 staining on the indicated PEL cell lines and control WSU-NHL cell line. Data were obtained by acquiring  $1 \times 10^4$  cells stained with the anti-CD30-fluorescein isothiocyanate (FITC) antibody. Blue line indicates CD30-stained cell population and black line indicates background fluorescence observed with isotype control. (B-D) CD30 expression in primary PEL cells. Malignant cells from PEL patient (case 1) are highlighted with Papanicolaou stain (I). Immunocytochemistry analysis shows positive staining for epithelial membrane antigen (EMA) (II), HHV-8 latent antigen LANA (nuclear stain) (III), and CD30 (IV). Original magnification: I, III, IV  $\times 100$  and II  $\times 50$ . (C) Large and discohesive malignant cells from PEL patient (case 2) are highlighted with hematoxylin and eosin stain (I). Immunocytochemistry analysis shows positive staining for EMA (II), HHV-8 latent antigen LANA (nuclear stain) (III), and CD30 (IV). Original magnification: I-IV  $\times 100$ . (D) Top shows hematoxylin and eosin staining of PEL patient (case 3) lymphoma cells and bottom shows an immunohistochemistry stain for CD30 in neoplastic cells of the same PEL patient. Original magnification  $\times 600$ .

(Figure 2B-C). A total of 8 of 9 cases strongly expressed surface CD30. Overall, these findings confirm that the majority of PEL tumors express surface CD30.

#### In vitro brentuximab vedotin treatment blocks proliferation of PEL cells

After demonstrating widespread expression of CD30 on PEL cell lines and primary tumors (Figure 2), we hypothesized that brentuximab vedotin may effectively target and kill PEL cells. To this end, we examined its effects on cell proliferation. Treatment of BC1, BC3, UM-PEL-1c, and UM-PEL-3c cells with increasing concentrations of brentuximab vedotin led to a significant decrease in proliferation of all the analyzed cell lines, although the cell lines had different sensitivity to the treatment (Figure 3). Brentuximab vedotin treatment resulted in a significant block in proliferation of BC-1 cells at  $100 \mu\text{g/mL}$  compared with untreated control at 72 hours ( $P < .001$ ) (Figure 3A). In BC-3 cells, brentuximab vedotin led to proliferative arrest at a concentration of  $1 \mu\text{g/mL}$  and  $10 \mu\text{g/mL}$  ( $P = .001$  and  $P < .0001$ , respectively) (Figure 3B). Similarly, we observed a profound inhibition in proliferation of UM-PEL-1c and UM-PEL-3c cells upon treatment with brentuximab vedotin at higher doses (Figure 3C-D). Although high doses of brentuximab vedotin were required to achieve desirable effects on cell proliferation in vitro, the

cytotoxicity was specific and selective, because the equivalent concentration of isotype-matched irrelevant Ig-vcMMAE control had a nominal effect on the proliferation of PEL cell lines (supplemental Figure 2).

#### Brentuximab vedotin induces G2/M arrest in PEL cells

Previous studies have shown that brentuximab vedotin acts by inhibiting microtubule spindle formation during the G2/M phase of the cell cycle in HL and ALCL cell lines.<sup>16</sup> To assess whether this phenomenon holds true in PEL, we examined the effect of brentuximab vedotin on the cell cycle profile of BC-1, BC-3, UM-PEL-1c, and UM-PEL-3c. Each cell line was treated with increasing concentrations of brentuximab vedotin ( $0$ - $100 \mu\text{g/mL}$ ). At 24 hours after treatment, cells were labeled with propidium iodide to measure total DNA content followed by flow cytometry analysis to determine cell cycle distribution. The percentage of the total population found in each phase of the cell cycle as obtained from flow histograms is indicated in Figure 4. In contrast to untreated control, cells exposed to  $100 \mu\text{g/mL}$  brentuximab vedotin showed a dramatic increase in the G2 cellular fraction (from  $45.85\%$  to  $72.15\%$  in BC-1 cells and from  $44.45\%$  to  $62.8\%$  in BC-3 cells) with a concomitant decrease in the fraction of G1 cells (Figure 4A-B). Brentuximab vedotin-induced G2 arrest was also observed in UM-PEL-1c and UM-PEL-3c as indicated

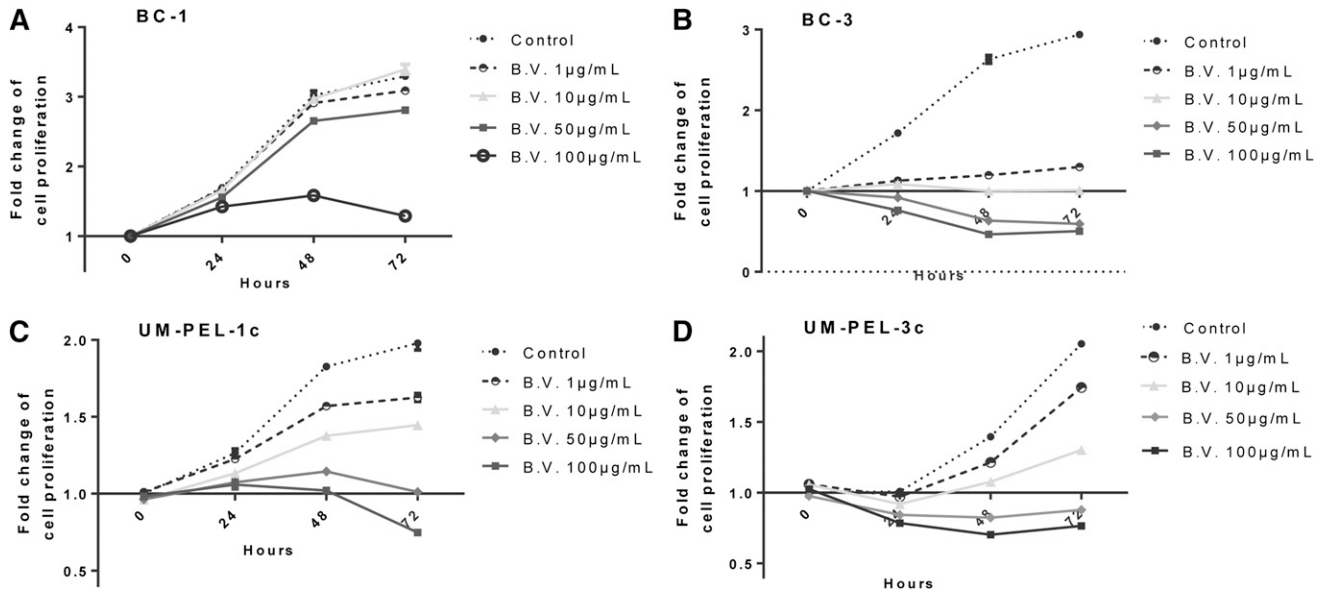


**Figure 3. Brentuximab vedotin blocks proliferation of PEL cells.** Human PEL cell lines BC-1 (A), BC-3 (B), UM-PEL-1c (C), and UM-PEL-3c (D) were treated with brentuximab vedotin (B.V.) at indicated doses for 0, 24, 48, and 72 hours. Proliferative response at each time point was measured by MTS assay. Results are shown as fold change of proliferation compared with time 0 hours. Experiments depicted in panels A-D were repeated thrice independently in triplicate. The representative data from one experiment are shown. Error bars correspond to standard error of mean in all graphs.

by a rise in the number of cells in the G2/M phase (from 15.87% to 32% and from 26% to 45%, respectively) (Figure 4C-D). Furthermore, the effect was specific, because cell cycle arrest was not observed after sustained exposure to equivalently high concentrations of isotypically-matched irrelevant Ig-vcMMAE control (supplemental

Figure 3). Of note, a larger proportion of untreated BC-1 and BC-3 cells compared with UM-PEL-1c and UM-PEL-3c were in the G2/M phase; thus, the increase in the number of cells in the G2/M phase was less pronounced in the BC-1 and BC-3 cells compared with the UM-PEL-1c and UM-PEL-3c lines. Overall, these data demonstrate

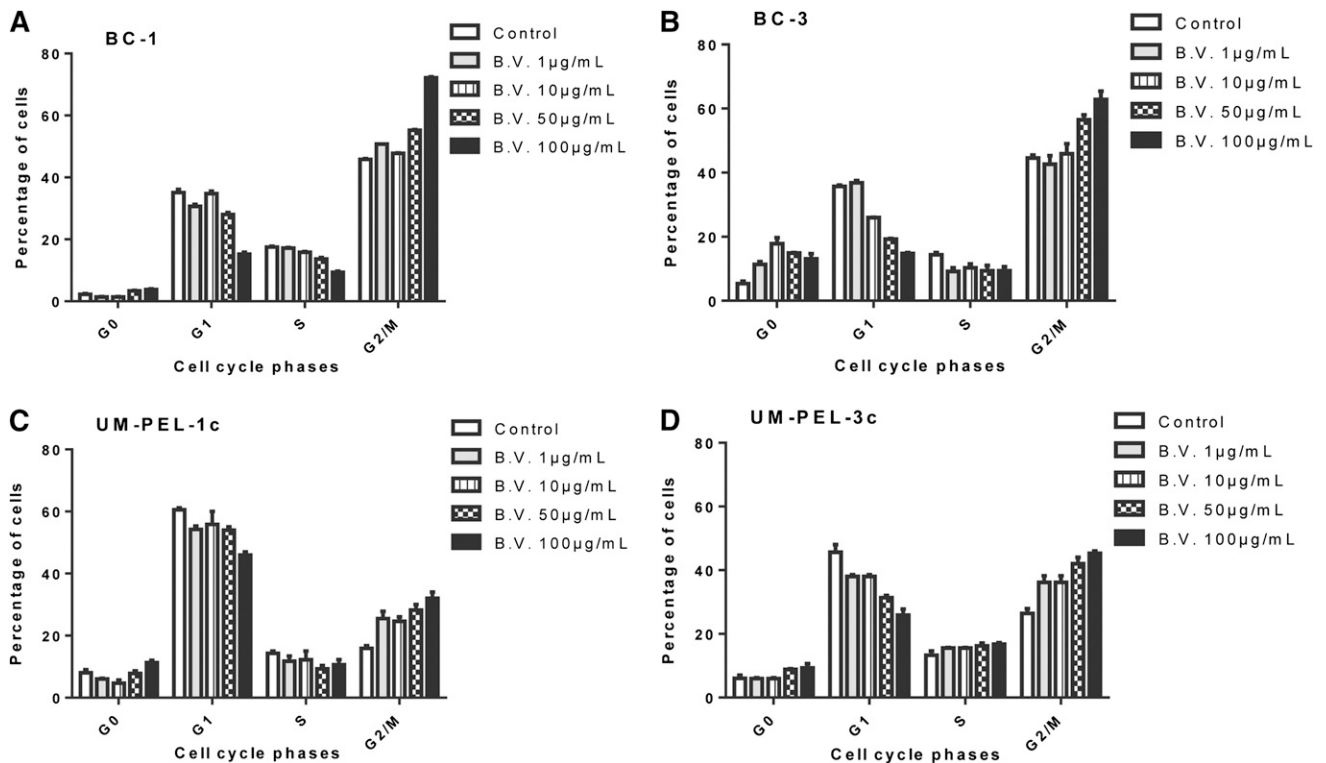


**Figure 4. Brentuximab vedotin induces G2/M cell cycle arrest of PEL cells.** PEL cell lines BC-1 (A), BC-3 (B), UM-PEL-1c (C), and UM-PEL-3c (D) were treated with brentuximab vedotin (B.V.) at increasing concentrations. At 24 hours after treatment, cells were stained with propidium iodide to measure DNA content and analyzed by flow cytometry for cell cycle distribution. Bar graphs indicate the percentage of cells in different phases of cell cycle (G0, G1, S, G2/M). Experiments depicted in panels A-D were repeated thrice independently in triplicate. The representative data from one experiment are shown. Error bars correspond to standard error of the mean in all graphs.

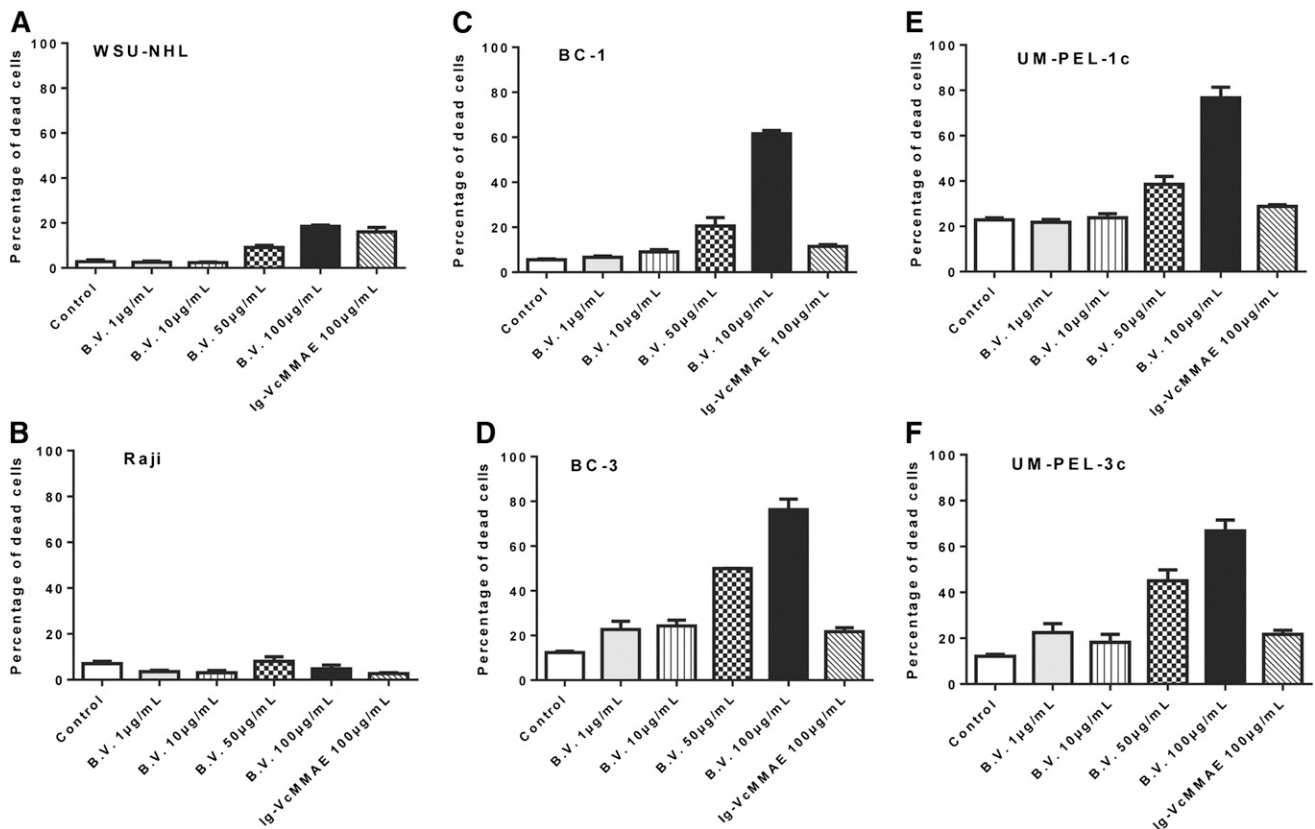


**Figure 5. Brentuximab vedotin triggers apoptosis of PEL cells.** Lymphoma cell lines lacking CD30 expression WSU-NHL (A) and Raji (B) and CD30-expressing PEL cell lines BC-1 (C), BC-3 (D), UM-PEL-1c (E), and UM-PEL-3c (F) were treated with increasing concentrations of brentuximab vedotin (B.V.) or Ig-VcMMAE. At 72 hours after treatment, cell viability was determined by flow cytometry following YO-PRO and propidium iodide staining. Experiments depicted in panels A-E were repeated thrice independently in triplicate. The representative data from one experiment are shown. Error bars correspond to the standard error of the mean in all graphs.

that brentuximab vedotin selectively induced cell cycle arrest in the G2/M phase in all analyzed PEL cell lines, similar to its effects in other CD30-expressing tumor lines.<sup>16</sup>

#### Brentuximab vedotin triggers apoptosis of PEL cells

Having shown the effects of brentuximab vedotin on the viability and cell cycle of PEL cells, we next examined its effects on cellular apoptosis. Increased apoptosis was observed in all 4 analyzed PEL cell lines at 50 µg/mL and 100 µg/mL after 72 hours, as illustrated in Figure 5. Relative to untreated controls or an equivalent concentration of isotype-matched irrelevant Ig-vcMMAE control, BC-1, BC-3, UM-PEL-1c, and UM-PEL-3c cells showed a 56%, 63.9%, 53.88%, and 54.62% increase in apoptotic cells following exposure to brentuximab vedotin, respectively (Figure 5C,F). Furthermore, brentuximab vedotin failed to induce the cell death in CD30-negative WSU-NHL and Raji cells at equivalent concentrations (Figure 5A-B). This suggested that the observed apoptotic effects were restricted to CD30-expressing cells (Figure 5A-B) and eliminated the possibility of nonspecific cytotoxicity from brentuximab vedotin treatment. Taken together, these studies show that brentuximab vedotin exerts potent and specific cytotoxic effects on all the analyzed CD30-expressing PEL cell lines, although at higher in vitro concentrations than in ALCL cell lines (supplemental Figure 4).

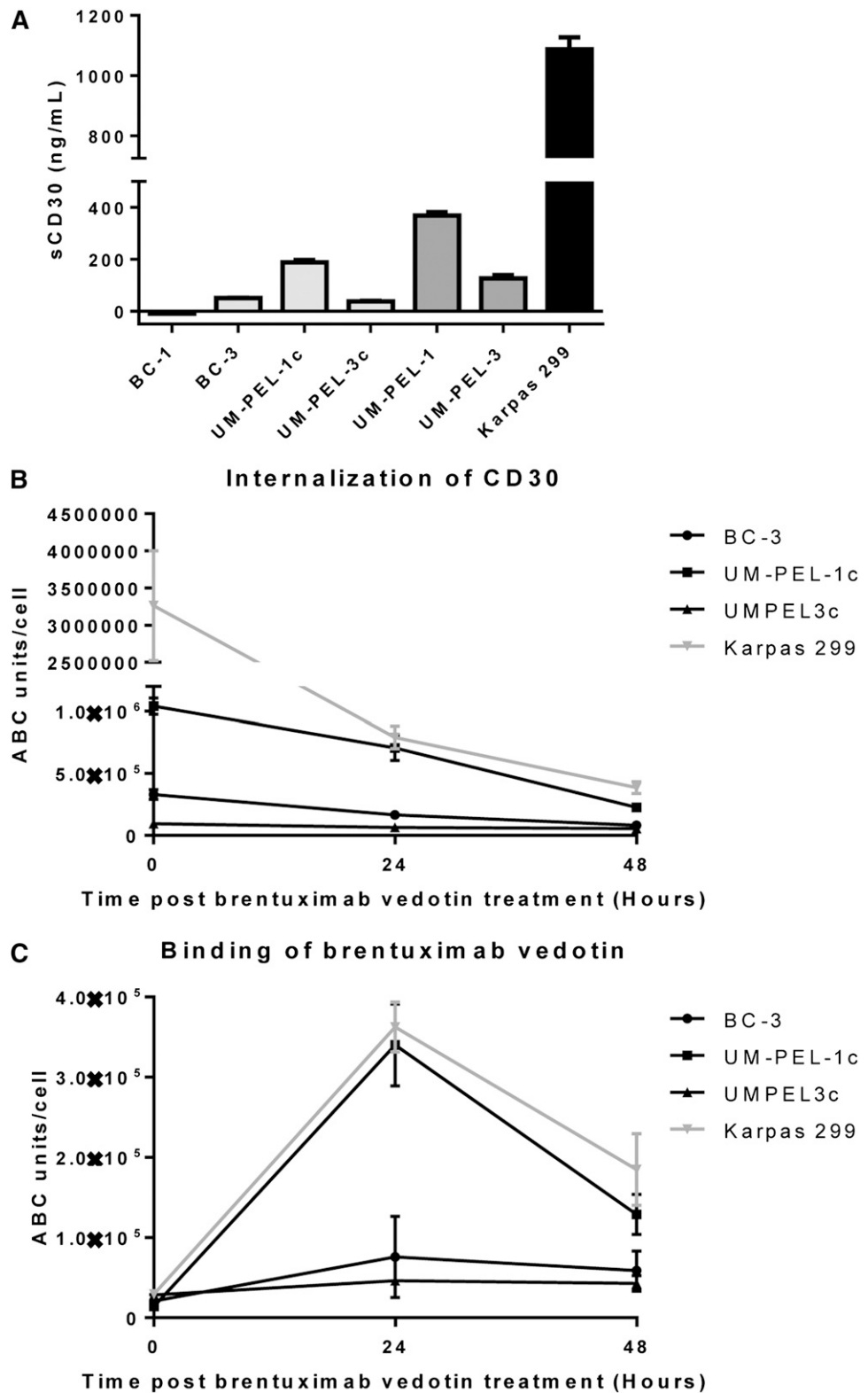
The requirement for higher brentuximab vedotin concentrations in the PEL cell lines to achieve similar cytotoxic effects as observed in the ALCL cell lines might be attributed to differences in the levels of soluble CD30 (sCD30) that is cleaved by metalloproteases from

the cell surface and may decrease brentuximab vedotin binding to the cell surface of CD30. However, higher sCD30 levels were observed in the more sensitive Karpas 299 ALCL cell line compared with the analyzed PEL cell lines (Figure 6A). Alternatively, the observed differences might stem from different surface CD30 expression, leading to diminished brentuximab vedotin cell surface binding and/or decreased intracellular uptake. To address these possibilities, we compared cell surface CD30 expression, binding of brentuximab vedotin, and its internalization into the cells. We measured and calculated the antigen-binding capacity per cell of anti-CD30 and anti-hIgG antibodies in PEL (BC-3, UM-PEL-1c, UM-PEL-3c) and ALCL (Karpas 299) cell lines, exposed to 15 µg/mL brentuximab vedotin at initial time point (0) and at 24 and 48 hours. Karpas 299 expressed higher initial surface CD30 levels compared with the analyzed PEL cell lines (supplemental Figure 4). Over time, surface CD30 internalization occurred faster and more extensively in the Karpas 299 vs analyzed PEL cell lines (Figure 6B). Concordantly, greater surface brentuximab vedotin cell surface binding was observed at 24 and 48 hours in the Karpas 299 vs most of the analyzed PEL cell lines, with the exception of UM-PEL-1c (Figure 6C). These findings may also explain the higher in vitro sensitivity of the UM-PEL-1c and BC-3 compared with the UM-PEL-3c cell line.

#### Brentuximab vedotin treatment does not affect KSHV lytic and latent gene transcription

Various chemotherapeutic agents targeting PEL are known to induce the viral lytic cycle, which may contribute to the death of the cells

**Figure 6. sCD30 levels, CD30 internalization, and brentuximab vedotin cell surface binding.** (A) sCD30 levels measured by ELISA in indicated cell lines and in cells directly derived from mice ascites. Error bar represents standard error of the mean between triplicate wells. (B) Cell surface CD30 expression and (C) cell surface brentuximab vedotin binding. BC-3, UM-PEL-1c, UM-PEL-3c, and Karpas 299 cells were incubated with 15  $\mu\text{g/mL}$  brentuximab vedotin for 0, 24, and 48 hours followed by incubation with anti-CD30 (fluorescein isothiocyanate [FITC]) (B) or anti-hIgG (FITC) (C) to determine antigen-binding capacity values for CD30 (B) and of bound brentuximab vedotin (C), respectively. Microbeads coated with known quantities of mouse-IgG were incubated with saturating quantities of anti-CD30 (FITC) or anti-hIgG (FITC) antibodies to determine mean fluorescence intensity assessed by flow cytometry to obtain standard curves. Data are representative of 3 independent experiments and error bars correspond to the standard error of the mean.



Downloaded from http://ashpublications.net/blood/article-pdf/122/7/1233/1374010/1233.pdf by guest on 02 June 2024

by the lytically replicating virus.<sup>9,27,28</sup> Therefore, we examined by qRT-PCR the levels of latent and lytic KSHV transcripts in UM-PEL-1c treated with increasing concentrations of brentuximab vedotin. Brentuximab vedotin treatment did not alter transcript levels of latent gene (LANA) (supplemental Figure 6A). IE lytic

(RTA), delayed early lytic (vGPCR), and late lytic (K8.1) transcripts were also not induced upon treatment with brentuximab vedotin (supplemental Figures 6B and 5D). These findings suggest that brentuximab vedotin-induced apoptosis is independent of KSHV gene transcription and induction of lytic replication.

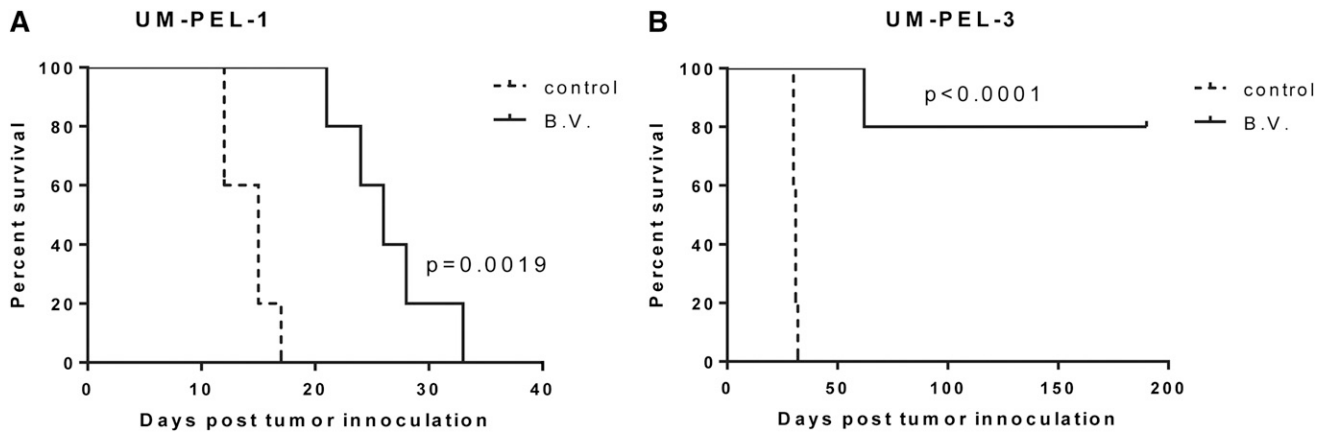


**Figure 7. Brentuximab vedotin extends the survival of PEL xenograft mice.** Kaplan-Meier survival curves of PEL xenograft mice. NOD/SCID mice ( $n = 5/\text{group}$ ) were injected with  $25 \times 10^6$  UM-PEL-1 (A) and UM-PEL-3 (B) cells. At 3 days postinjection, mice were treated for 3 weeks with interperitoneal injections of brentuximab vedotin (B. V.), PBS, or isotype-matched irrelevant Ig-vcMMAE. Only one control group is shown, because mice in both groups exhibited identical Kaplan-Meier survival curves. Results are representative of 2 independent experiments.

### Brentuximab vedotin induces in vivo regression of PEL xenograft tumors

The proapoptotic activity of brentuximab vedotin against PEL cell lines suggests that this therapeutic approach could be useful for treating patients. To evaluate the effects of brentuximab vedotin in vivo, groups of NOD/SCID mice were inoculated into the peritoneal cavity with UM-PEL-1 or UM-PEL-3 cells. On the third day after interperitoneal injection, tumor-bearing mice were treated interperitoneally with PBS, isotype-matched irrelevant Ig-vcMMAE control, or brentuximab vedotin. All treatments were given thrice weekly for 3 weeks and mice were monitored on a daily basis. In vivo treatment of the UM-PEL-1 and UM-PEL-3-bearing mice with brentuximab vedotin (3 mg/kg) was well tolerated and improved overall survival. UM-PEL-1 tumor-bearing mice treated with brentuximab vedotin had a median survival of 26 days compared with 15 days in the controls ( $P < .01$ ) (Figure 7A). Four of five UM-PEL-3-injected animals remained tumor free for more than 6 months compared with a median survival of 30 days for control mice (UM-PEL-3:  $P < .0001$ ) (Figure 7B). The remaining mouse redeveloped ascites during the follow-up, yet still showed a clear survival advantage over control mice. There was no difference in the outcome of mice treated with PBS and isotype-matched irrelevant Ig-vcMMAE control, indicating that the observed therapeutic responses were specific for the CD30 targeted agent. In both tumor models, brentuximab vedotin-treated mice showed no signs or symptoms of toxicity at the used therapeutic doses, which were significantly lower than the reported maximum tolerated dose.<sup>16</sup> Taken together, brentuximab vedotin demonstrated significant antitumor activity in 2 different xenograft models of PEL at doses similar to those previously shown to be active in ALCL xenograft models.<sup>16</sup>

## Discussion

Development of new therapies for PEL has been delayed due to the lack of a suitable model system that mimics human disease. The tumor microenvironment contributes to the canonical growth of PEL cells. Hence, in vitro cell culture condition may alter KSHV and host gene expression signatures from patterns that are observed in vivo.<sup>29</sup> Consequently, available PEL cell lines may not reliably represent

KSHV biology. For this reason, we previously developed the UM-PEL-1 cell line and mouse model by directly transplanting PEL cells collected from a patient into the peritoneal cavities of NOD/SCID mice without ex vivo culture. We have previously shown that by abolishing ex vivo culture steps, these cells better reflect the in vivo characteristic of the disease and eliminate culture-induced changes in KSHV gene expression.<sup>9</sup> Herein, by using a similar methodology, we have developed another PEL mouse model (UM-PEL-3) that, together with the UM-PEL-1 model, will allow better interrogation of PEL biology and pathogenesis and permit a more comprehensive assessment of the efficacy of new therapeutic approaches.

Low incidence of PEL prevents the conduct of large-scale clinical trials. As a result, an optimized therapeutic regimen for PEL has remained elusive but is urgently needed, because PEL patients survive on average only 6 months with currently available therapies. Considering these factors, it is imperative that PEL clinical trials have a focused approach and include only therapies with the highest likelihood of success. Reliable PEL animal models may facilitate the screening and proper selection of promising therapeutic approaches for PEL patients. Herein, using phenotypically reliable PEL mouse models as well as available cell lines and primary tumors, we demonstrate that targeting CD30 with brentuximab vedotin is a therapeutic approach for PEL that warrants clinical investigation.

Previous studies demonstrated that brentuximab vedotin exhibits cytotoxic effects in HL and ALCL cell lines and induces cell cycle arrest in the G2/M phase.<sup>16</sup> Targeted in vitro delivery of MMAE to CD30-expressing cells with brentuximab vedotin led to high and sustained intracellular MMAE levels, inducing death of both CD30-expressing malignant cells and neighboring malignant cells that do not express the target antigen.<sup>30</sup> In vivo brentuximab vedotin therapy demonstrated antitumor effects against a subcutaneous model of ALCL using Karpas 299 cells and the HL cell line L540, as well as in a disseminated Karpas 299 ALCL tumor model in SCID mice at doses as low as 1 mg/kg. Herein, we demonstrate that in vitro treatment with brentuximab vedotin inhibits cell proliferation by inducing G2/M arrest and apoptosis in multiple PEL cell lines, although at concentrations higher than those observed in the HL and ALCL cell lines. Our studies suggest that higher surface CD30 expression on the ALCL may predispose to greater cell surface brentuximab vedotin binding, which in association with faster and greater intracellular uptake may lead to greater sensitivity in the ALCL cell lines. However, higher concentrations of



brentuximab vedotin could compensate for these biological differences and lead to similar cytotoxicity in PEL cell lines, suggesting that the final amounts of MMAE delivered to each cell were sufficient to induce cell apoptosis and death. Moreover, the antiproliferative effect was specific for PEL cells and mediated by CD30 targeting, because an equivalent concentration of isotype-matched irrelevant Ig-vcMMAE control failed to elicit any such response. Furthermore, in vivo brentuximab vedotin significantly extended the survival of PEL-bearing mice at doses of 3 mg/kg, which is similar to doses shown to be effective in the HL and ALCL xenograft models. Additionally, 4 of 5 UM-PEL-3 xenograft mice receiving therapy remained disease free for 200 days post treatment, which is almost identical to the survival curves obtained for disseminated Karpas 299 ALCL tumor with the same treatment.<sup>16</sup> The PEL animals receiving the treatment did not demonstrate any signs of toxicity in concordance with previous reports demonstrating that immunodeficient mice treated with 30 mg/kg brentuximab vedotin showed no signs of toxicity<sup>16</sup> and with a maximum tolerated dose of ~100 mg/kg in immunocompetent mice strains.<sup>31</sup> The marked differences in the in vivo and in vitro doses of the brentuximab vedotin needed to achieve cytotoxic effects may be attributed to previously reported differences in biological behavior between PEL cells grown in culture and those in humans or animals, further emphasizing the importance of evaluating drug efficacy using reliable and representative PEL models. The mechanisms underlying these in vitro and in vivo brentuximab vedotin sensitivity differences are currently unknown. However, it is possible that differences in rates of intracellular trafficking, enzymatic cleavage, and release of MMAE from the lysosome may be the factors responsible for the observed difference.

The preclinical studies in HL and ALCL led to a subsequent evaluation of the efficacy of brentuximab vedotin in patients with relapsed/refractory HL and systemic ALCL. Data obtained from clinical trials demonstrated that brentuximab vedotin is an effective therapy in these patients, leading to responses in ~70% of cases.<sup>19-21</sup> The treatment regimen demonstrated a reasonable toxicity profile and durable remissions in a portion of the responders, paving the way for accelerated approval of medication by the Food and Drug Administration.<sup>19</sup> Moreover, the compelling antitumor activity of brentuximab vedotin was recently demonstrated in patients with relapsed or refractory CD30-positive NHLs, in particular diffuse large B-cell lymphoma, angioimmunoblastic T-cell lymphoma, and

gray zone lymphoma.<sup>32</sup> Interestingly, there was marked variability in the surface CD30 expression levels between patients that demonstrated clinical responses. The preclinical brentuximab vedotin efficacy in PEL cell lines and mouse models reported here is similar to what was previously observed in preclinical studies in HL and ALCL. Because subsequent clinical studies demonstrated brentuximab vedotin activity in HL and ALCL patients, the observations reported herein provide a strong basis to evaluate brentuximab vedotin as a therapy for PEL patients in clinical trials.

## Acknowledgments

The authors thank Seattle Genetics for providing brentuximab vedotin and Ig-vcMMAE for these studies and George McNamara, Director of the Analytical Imaging Core Facility at the University of Miami Diabetes Research Institute, for expert assistance in immunofluorescence studies.

I.S.L. is supported by National Institutes of Health grants NIH National Cancer Institute CA109335, NIH CA122105, and U56 CA112973, and by the Dwoskin Family and Recio Family Foundations. E.A.M. is supported by NIH National Cancer Institute grant CA136387. J.C.R. is supported by AIDS Malignancies consortium NIH National Cancer Institute grant U01 CA 1Z1947.

## Authorship

Contribution: S.B. performed most of the laboratory work, analyzed data, and wrote the paper; B.M.A., Y.N., V.S., and J.R.C. performed laboratory experiments; J.C.R. and E.A.M. provided reagents and analyzed the data; and I.S.L. conceptualized the idea of the study, supervised the experiments, analyzed the data, provided funding, and wrote the paper.

Conflict-of-interest disclosure: The authors declare no competing financial interests.

Correspondence: Izidore S. Lossos, University of Miami, Sylvester Comprehensive Cancer Center, Division of Hematology and Oncology, 1475 NW 12th Ave (D8-4), Miami, FL 33136; e-mail: ilossos@med.miami.edu.

## References

- Cesarman E, Chang Y, Moore PS, Said JW, Knowles DM. Kaposi's sarcoma-associated herpesvirus-like DNA sequences in AIDS-related body-cavity-based lymphomas. *N Engl J Med*. 1995;332(18):1186-1191.
- Jones D, Ballestas ME, Kaye KM, et al. Primary effusion lymphoma and Kaposi's sarcoma in a cardiac-transplant recipient. *N Engl J Med*. 1998;339(7):444-449.
- Nador RG, Cesarman E, Chadburn A, et al. Primary effusion lymphoma: a distinct clinicopathologic entity associated with the Kaposi's sarcoma-associated herpes virus. *Blood*. 1996;88(2):645-656.
- Arvanitakis L, Mesri EA, Nador RG, et al. Establishment and characterization of a primary effusion (body cavity-based) lymphoma cell line (BC-3) harboring kaposi's sarcoma-associated herpesvirus (KSHV/HHV-8) in the absence of Epstein-Barr virus. *Blood*. 1996;88(7):2648-2654.
- Chang Y, Cesarman E, Pessin MS, et al. Identification of herpesvirus-like DNA sequences in AIDS-associated Kaposi's sarcoma. *Science*. 1994;266(5192):1865-1869.
- Cesarman E, Mesri EA. Kaposi sarcoma-associated herpesvirus and other viruses in human lymphomagenesis. *Curr Top Microbiol Immunol*. 2007;312:263-287.
- Mesri EA, Cesarman E, Boshoff C. Kaposi's sarcoma and its associated herpesvirus. *Nat Rev Cancer*. 2010;10(10):707-719.
- Grundhoff A, Ganem D. Inefficient establishment of KSHV latency suggests an additional role for continued lytic replication in Kaposi sarcoma pathogenesis. *J Clin Invest*. 2004;113(1):124-136.
- Sarosiek KA, Cavallin LE, Bhatt S, et al. Efficacy of bortezomib in a direct xenograft model of primary effusion lymphoma. *Proc Natl Acad Sci USA*. 2010;107(29):13069-13074.
- Bhatt S, Ashlock BM, Toomey NL, et al. Efficacious proteasome/HDAC inhibitor combination therapy for primary effusion lymphoma. *J Clin Invest*. 2013;123(6):2616-2628.
- Dürkop H, Foss HD, Eitelbach F, et al. Expression of the CD30 antigen in non-lymphoid tissues and cells. *J Pathol*. 2000;190(5):613-618.
- Chiarle R, Podda A, Prolla G, Thorbecke GJ, Inghirami G. CD30 in normal and neoplastic cells. *Clin Immunol*. 1999;90(2):157-164.
- Dürkop H, Latza U, Hummel M, Eitelbach F, Seed B, Stein H. Molecular cloning and expression of a new member of the nerve growth factor receptor family that is characteristic for Hodgkin's disease. *Cell*. 1992;68(3):421-427.
- Falini B, Pileri S, Pizzolo G, et al. CD30 (Ki-1) molecule: a new cytokine receptor of the tumor necrosis factor receptor superfamily as a tool for diagnosis and immunotherapy. *Blood*. 1995;85(1):1-14.
- King HD, Dubowchik GM, Mastalerz H, et al. Monoclonal antibody conjugates of doxorubicin prepared with branched peptide linkers: inhibition of aggregation by methoxytriethyleneglycol chains. *J Med Chem*. 2002;45(19):4336-4343.

16. Francisco JA, Cerveny CG, Meyer DL, et al. cAC10-vcMMAE, an anti-CD30-monomethyl auristatin E conjugate with potent and selective antitumor activity. *Blood*. 2003;102(4):1458-1465.
17. Senter PD, Sievers EL. The discovery and development of brentuximab vedotin for use in relapsed Hodgkin lymphoma and systemic anaplastic large cell lymphoma. *Nat Biotechnol*. 2012;30(7):631-637.
18. Oflazoglu E, Kissler KM, Sievers EL, Grewal IS, Gerber HP. Combination of the anti-CD30-auristatin-E antibody-drug conjugate (SGN-35) with chemotherapy improves antitumor activity in Hodgkin lymphoma. *Br J Haematol*. 2008;142(1):69-73.
19. Younes A, Gopal AK, Smith SE, et al. Results of a pivotal phase II study of brentuximab vedotin for patients with relapsed or refractory Hodgkin's lymphoma. *J Clin Oncol*. 2012;30(18):2183-2189.
20. Younes A, Bartlett NL, Leonard JP, et al. Brentuximab vedotin (SGN-35) for relapsed CD30-positive lymphomas. *N Engl J Med*. 2010;363(19):1812-1821.
21. de Claro RA, McGinn K, Kwitkowski V, et al. U.S. Food and Drug Administration approval summary: brentuximab vedotin for the treatment of relapsed Hodgkin lymphoma or relapsed systemic anaplastic large-cell lymphoma. *Clin Cancer Res*. 2012;18(21):5845-5849.
22. Mohamed AN, al-Katib A. Establishment and characterization of a human lymphoma cell line (WSU-NHL) with 14;18 translocation. *Leuk Res*. 1988;12(10):833-843.
23. Cesarman E, Moore PS, Rao PH, Inghirami G, Knowles DM, Chang Y. In vitro establishment and characterization of two acquired immunodeficiency syndrome-related lymphoma cell lines (BC-1 and BC-2) containing Kaposi's sarcoma-associated herpesvirus-like (KSHV) DNA sequences. *Blood*. 1995;86(7):2708-2714.
24. Fromm JR, McEarchern JA, Kennedy D, Thomas A, Shustov AR, Gopal AK. Clinical binding properties, internalization kinetics, and clinicopathologic activity of brentuximab vedotin: an antibody-drug conjugate for CD30-positive lymphoid neoplasms. *Clin Lymphoma Myeloma Leuk*. 2012;12(4):280-283.
25. Piris M, Brown DC, Gatter KC, Mason DY. CD30 expression in non-Hodgkin's lymphoma. *Histopathology*. 1990;17(3):211-218.
26. Sabattini E, Bacci F, Sagranso C, Pileri SA. WHO classification of tumours of haematopoietic and lymphoid tissues in 2008: an overview. *Pathologica*. 2010;102(3):83-87.
27. Klass CM, Krug LT, Pozharskaya VP, Offermann MK. The targeting of primary effusion lymphoma cells for apoptosis by inducing lytic replication of human herpesvirus 8 while blocking virus production. *Blood*. 2005;105(10):4028-4034.
28. Wu FY, Tang QQ, Chen H, et al. Lytic replication-associated protein (RAP) encoded by Kaposi sarcoma-associated herpesvirus causes p21CIP-1-mediated G1 cell cycle arrest through CCAAT/enhancer-binding protein- $\alpha$ . *Proc Natl Acad Sci USA*. 2002;99(16):10683-10688.
29. Staudt MR, Kanan Y, Jeong JH, Papin JF, Hines-Boykin R, Dittmer DP. The tumor microenvironment controls primary effusion lymphoma growth in vivo. *Cancer Res*. 2004;64(14):4790-4799.
30. Okeley NM, Miyamoto JB, Zhang X, et al. Intracellular activation of SGN-35, a potent anti-CD30 antibody-drug conjugate. *Clin Cancer Res*. 2010;16(3):888-897.
31. Hamblett KJ, Senter PD, Chace DF, et al. Effects of drug loading on the antitumor activity of a monoclonal antibody drug conjugate. *Clin Cancer Res*. 2004;10(20):7063-7070.
32. Jacobsen ED, Advani RH, Oki Y, et al. A phase 2 study of brentuximab vedotin in patients with relapsed or refractory cd30-positive non-Hodgkin lymphomas: interim results [abstract]. *Blood*. 2012;120(21). Abstract 2746.